IUST
Iran University of Science and Technology

Iranian Journal of Electrical and Electronic Engineering

Journal Homepage: ijeee.iust.ac.ir

Research Paper

Distributed Nonlinear Robust Control for Power Flow in Islanded Microgrids

S. M. Hoseini*, N. Vasegh*(C.A.), and A. Zangeneh*

Abstract: In this paper, a robust local controller has been designed to balance the power for distributed energy resources (DERs) in an islanded microgrid. Three different DER types are considered in this study; photovoltaic systems, battery energy storage systems, and synchronous generators. Since DER dynamics are nonlinear and uncertain, which may destabilize the power system or decrease the performance, distributed robust nonlinear controllers are designed for the DERs. They are based on the Lyapunov stabilization theory and super-twisting integral sliding mode control which guarantees system stability and optimality simultaneously. The reference signals for each DER are generated by a supervisory controller as a power management system. The controllers proposed in this work are robust, have fast response times, and most importantly, the control signals satisfy physical system constraints. The designed controller stability and effectiveness are also verified using numerical simulations.

Keywords: Islanded Microgrid, Photovoltaic System, Synchronous Generator, Battery Energy Storage System, Distributed Nonlinear Robust Controller, Super-Twisting Integral Sliding Mode Control, Lyapunov Theory.

1 Introduction

DUE to increasing electrical power demand, renewable energy sources have to be adopted into modern power grids. The most common resources implemented are solar, wind, and hydroelectric [1]. Renewable energy resources and energy storage systems can form a microgrid. These grids can operate in islanded, disconnected from the main power grid, or grid-connected mode. In the first mode, large voltage or frequency fluctuations can result in blackouts; hence it is necessary for an islanded microgrid to regulate its voltage and frequency.

Voltages and frequencies in islanded microgrids only depend on the distributed energy resources (DERs) connected to it. Therefore, the dynamics of each DER become very important for islanded microgrid voltage and frequency regulations [2]. A common simplifying assumption made in islanded microgrid studies is that DERs are ideal and non-dynamic. As a result, initial phase voltages and frequencies are expected to be their corresponding desired values; in addition, the control input for an islanded microgrid is assumed to be the DER terminal voltage. Hence, a linear controller for islanded microgrid stabilization is only logical when linear loads are considered. For instance, in [3] a linear H_∞ controller is used to stabilize a master DER to regulate the microgrid voltage, as proportional-integral (PI) controllers are adopted to regulate slave DERs currents. In [4] where only one DER is considered in the microgrid, unmodeled dynamics were considered as system uncertainties, and the authors designed an H_∞ controller to attenuate the unmodeled dynamics effects on the system output. Another conventional assumption made considering microgrids is parallel loads [3, 4]. In [5, 6] a radial structured microgrid is regarded and a robust controller is designed for the linear system model. In [7], robust frequency control of an islanded microgrid is considered; the uncertain dynamics are assumed to be linear and standard H_∞ and μ-synthesis approaches are used to design the control law. Linear controllers, e.g. the controllers in [3-7], only stabilize nonlinear systems locally and there is no guarantee for global stability. Therefore, it is important to consider the DER nonlinear model and design appropriate controllers to provide

Iranian Journal of Electrical and Electronic Engineering, 2020.
Paper first received 01 March 2019, revised 25 August 2019, and accepted 28 August 2019.
* The authors are with the Faculty of Electrical Engineering, University of Shahid Rajaee Teacher Training, Tehran, Iran.
E-mails: m.hoseini@sru.ac.ir, n.vasegh@sru.ac.ir, and a.zangeneh@sru.ac.ir.
Corresponding Author: N. Vasegh.

global stability. Thus, the system investigated in the present study is not linearized and DER dynamics are considered.

In [2] an islanded microgrid is assumed with two photovoltaic systems (PVs) and two battery energy storage systems (BESSs) which are connected to the microgrid by three-phase inverters. The control inputs of inverters are basically several switches. Considering the nonlinear dynamics of DERs, some nonlinear strategies like feedback linearization [2], [8-11], and sliding mode control (SMC) [12] are utilized to provide global microgrid stability. Although the inverter control signal is bounded, this aspect is normally omitted in controller design and stability analysis studies, e.g. [2], [8-10]. Considering the constraint on the control signal is absolutely necessary and if it is disregarded, the switches can even generate power with non-feasible control signals. The inverter control signals are either On or Off; using the pulse width modulation technique, the control signals vary within the [0, 1] interval. Here, this constraint is expressed as a constraint in the dq-frame.

There are some researches which deal with microgrid power management. The power management system generates the reference signals needed by the DGs to operate correctly. In [13], a decentralized method is used for load sharing and power management in an islanded microgrid. In [14], uncertainty is considered in the communication links; the authors tried to minimize the communications and derived a robust controller using the Lyapunov stability theory. However, in this manuscript, a simpler but more flexible method is presented; the ability to communicate with PVs for power management is assumed to be possible by adjusting reference signals to obtain maximum power.

In [15] a distributed model predictive secondary voltage control of islanded microgrids with feedback linearization is presented, where first, the nonlinear inverter-based DG dynamics are linearized by input-output feedback linearization method. Then, a linear distributed model predictive control (MPC) is adopted to implement secondary voltage control. Finally, a PI algorithm is used to realize frequency restoration and active power sharing. As linearizing dynamics can result in loss of valuable information, the proposed method in the present study does not linearize system dynamics and is further less computationally demanding as compared with methods like MPC.

Sedghi *et al.* [16] have designed a controller consisting of three cascade connected power, voltage and current controllers. The first controller is designed based on droop characteristics and the other two based on PI controllers. For performance validation, three scenarios considering load perturbation, disconnection of a DG, and nonlinear loads are investigated. Whereas, in this work, DG uncertainties are not considered.

Voltage and frequency regulations and active and reactive power sharing in islanded microgrids with renewable energy sources can be achieved by two-layer control strategies. This approach is attempted in [17], where the upper-level control determines the power generation references to minimize the overall voltage deviations while sharing the power. Also, the lower-level control adjusts the inverter output voltage magnitude and angle to track the power reference.

In this paper, distributed nonlinear robust controllers for PVs, BESSs, and synchronous generators (SGs) are designed. The proposed controllers based on Lyapunov and sliding mode strategies, systematically meet the input constraints. The SG is controlled based on super-twisting integral sliding mode strategy, which is a second-order SMC. The designed controllers are simulated separately and together in an islanded microgrid for illustration. In contrast to most studies where K_d and K_q limitations are disregarded in controller designs, these limitations are implemented in the present work and their effects on system stability are considered.

This paper is organized as follows. In Section 2, PV, BESS, and SG dynamical models are introduced. Controller design for each DER and their stability proofs are presented in Section 3. In Section 4, simulation results are provided to show the proposed controller performances. Finally, this paper is concluded and future works are presented in Section 5.

2 System Modeling

Here, nonlinear state-space models for PV, BESS, and SG are introduced in dq-frame. The microgrid studied in the present work consists of two PVs, two BESSs, one SG, and one consumer as illustrated in Fig. 1.

2.1 PV Model

The block diagram of a PV connected to a microgrid by a three-phase inverter is shown in Fig. 2. Also, its dynamical model can be expressed as follows [9]:

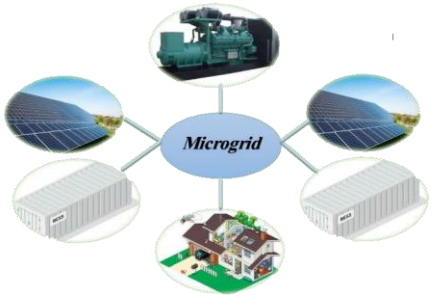

Fig. 1 A schematic of the microgrid studied.

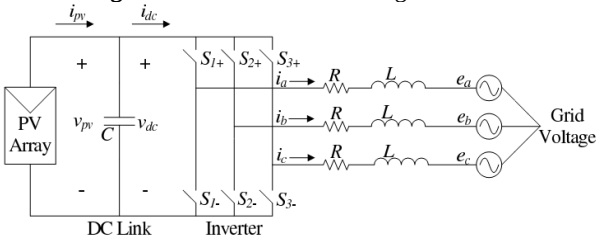

Fig. 2 PV block diagram connected to a microgrid by a three phase inverter [9].

$$\begin{cases} \dot{i}_a = -\frac{R}{L} i_a - \frac{1}{L} e_a + \frac{v_{PV}}{3L}\left(2K_a - K_b - K_c\right) \\ \dot{i}_b = -\frac{R}{L} i_b - \frac{1}{L} e_b + \frac{v_{PV}}{3L}\left(-K_a + 2K_b - K_c\right) \\ \dot{i}_c = -\frac{R}{L} i_c - \frac{1}{L} e_c + \frac{v_{PV}}{3L}\left(-K_a - K_b + 2K_c\right) \\ \dot{v}_{PV} = \frac{1}{C} i_{PV} - \frac{1}{C}\left(i_a K_a + i_b K_b + i_c K_c\right) \end{cases} \quad (1)$$

In (1), i_a, i_b, i_c, e_a, e_b, and e_c are three-phase currents and voltages, i_{pv} and v_{pv} are PV current and voltage, K_a, K_b, and K_c are inverter switch values (control inputs) which could be either zero or one, and R, L, and C are constant resistor, inductor and capacitor values, respectively. The PV voltage and current have an implicit static relation thoroughly explained in [18]. For the balanced three-phase microgrids, it is possible to transform the system (1) to dq-frame as follows:

$$\begin{cases} \dot{I}_d = -\frac{R}{L} I_d + \omega I_q - \frac{E_d}{L} + \frac{v_{PV}}{L} K_d \\ \dot{I}_q = -\omega I_d - \frac{R}{L} I_q - \frac{E_q}{L} + \frac{v_{PV}}{L} K_q \\ \dot{v}_{PV} = \frac{1}{C} i_{PV} - \frac{1}{C}\left(I_d K_d - I_q K_q\right) \end{cases} \quad (2)$$

where I_d, I_q, E_d, E_q, K_d, and K_q are currents, voltages, and control inputs in d and q directions, respectively. The transformation matrix from abc-frame to dq-frame is as follows:

$$P_{abc}^{dq} = \frac{2}{3}\begin{bmatrix} \cos(\theta) & \cos(\theta-120) & \cos(\theta+120) \\ \sin(\theta) & \sin(\theta) & \sin(\theta) \\ \frac{1}{2} & \frac{1}{2} & \frac{1}{2} \end{bmatrix} \quad (3)$$

where $\theta(t) = \omega(t) + \theta(0)$ is the rotating frame phase. In the dq-frame, active and reactive powers are determined using (4) and (5).

$$P = \frac{3}{2}\left(E_q I_q + E_d I_d\right) \quad (4)$$

$$Q = \frac{3}{2}\left(E_q I_d - E_d I_q\right) \quad (5)$$

Further, variables K_d and K_q are the new control inputs which can be computed by transforming the control signals from the abc-frame.

$$\begin{pmatrix} K_d \\ K_q \end{pmatrix} = \frac{2}{3}\begin{pmatrix} \cos(\theta)\left(K_a - \frac{1}{2}K_b - \frac{1}{2}K_c\right) + \sin(\theta)\left(\frac{\sqrt{3}}{2}K_b - \frac{\sqrt{3}}{2}K_c\right) \\ \sin(\theta)\left(K_a - \frac{1}{2}K_b - \frac{1}{2}K_c\right) - \cos(\theta)\left(\frac{\sqrt{3}}{2}K_b - \frac{\sqrt{3}}{2}K_c\right) \end{pmatrix} \quad (6)$$

As the variables K_a, K_b, and K_c belong within the [0, 1] interval, the control inputs K_d and K_q are bounded and this constraint cannot be omitted. Using (6), the signals K_a and K_b can be determined as follows.

$$\begin{pmatrix} K_a \\ K_b \end{pmatrix} = \begin{pmatrix} \sqrt{3}\left(K_d \sin\left(\theta + \frac{\pi}{3}\right) + K_q \sin\left(\theta - \frac{\pi}{3}\right)\right) + K_c \\ \sqrt{3}\left(K_d \sin(\theta) - K_q \cos(\theta)\right) + K_c \end{pmatrix} \quad (7)$$

The control signal bounds in the dq-frame are time-varying. Having time-invariant bounds on the control signals simplifies the design procedure. Assuming that K_d and K_q belong to the [–⅓, ⅓] interval, K_a, K_b, and K_c are guaranteed to always belong to the [0, 1] interval and the designed controller fulfills the input constraints of (7). The reverse transformation from the dq-frame to the abc-frame for the control signals might not be unique; based on $0 \le K_a, K_b, K_c \le 1$, and (7), one can conclude that $l_4 \le K_c \le l_3$ (defined by (8)-(9)) is acceptable. Thus, an acceptable range for K_c exists, which is proposed to be the average current value as shown in (10).

$$l_3 = \min\left(1 - l_1, 1 - l_2, 1\right) \quad (8)$$

$$l_4 = \max\left(-l_1, -l_2, 0\right) \quad (9)$$

$$K_c = \frac{l_3 + l_4}{2} \quad (10)$$

where,

$$l_1 = \sqrt{3}\left(K_d \sin\left(\theta + \frac{\pi}{3}\right) + K_q \sin\left(\theta - \frac{\pi}{3}\right)\right) \quad (11)$$

$$l_2 = \sqrt{3}\left(K_d \sin(\theta) - K_q \cos(\theta)\right) \quad (12)$$

Adopting (10), the control signals K_a and K_b can be uniquely determined by (7).

2.2 BESS Model

The BESS consists of a battery, a three-phase inverter for connecting to the microgrid, and an RLC filter. In dq-frame, the BESS model is quite similar to the PV and can be presented as the following [2]:

$$\begin{cases} \dot{I}_1 = \frac{1}{\tau_1}\left(M_d I_{bd} + M_q I_{bq} - I_1\right) \\ \dot{I}_{bd} = -\frac{R}{L} I_{bd} + \omega I_{bq} - \frac{E_d}{L} + \frac{v_{dc}}{L} M_d \\ \dot{I}_{bq} = -\omega I_{bd} - \frac{R}{L} I_{bq} - \frac{E_q}{L} + \frac{v_{dc}}{L} M_q \end{cases} \quad (13)$$

In (13), I_{bd}, I_{bq}, and I_1 are battery currents in dq-frame and its DC current respectively. M_d and M_q are the inverter switch signals in the dq-frame which have the same constraints as K_d and K_q in the PV model and the

v_{dc} is the I_1 dependent battery voltage [19]. Note that M_d and M_q are related and bounded; therefore, the stability analysis should be addressed by considering these constraints. Like PV, if a switch signal becomes greater than one it can be shown that the switch is generating and injecting power to the system, which is not possible. BESS active and reactive powers can be computed by (4) and (5).

2.3 SG Model

SG is widely used in microgrids as a reliable power source. A common SG model used in the current study is adapted from [20-21], where it is presented in dq-frame as,

$$\begin{cases} \dfrac{d\varphi_d}{dt} = \omega_e \varphi_q + r_s i_d + v_d \\ \dfrac{d\varphi_q}{dt} = -\omega_e \varphi_d + r_s i_q + v_q \\ \dfrac{d\varphi_f}{dt} = -r_f i_f + v_f \\ \dfrac{d\varphi_D}{dt} = -r_D i_D \\ \dfrac{d\varphi_Q}{dt} = -r_Q i_Q \\ \dfrac{d\delta}{dt} = \omega_e - \omega_0 \\ \dfrac{d\omega_e}{dt} = \dfrac{p}{J}\left(T_m - T_e\right) \end{cases} \tag{14}$$

where the following static relations between currents and fluxes are true.

$$\begin{cases} \varphi_d = -L_d i_d + m_{sf} i_f + m_{sD} i_D \\ \varphi_q = -L_q i_q + m_{sQ} i_Q \\ \varphi_f = L_f i_f + m_{fD} i_D - m_{sf} i_d \\ \varphi_D = L_D i_D + m_{fD} i_f - m_{sD} i_d \\ \varphi_Q = L_Q i_Q - m_{sQ} i_q \\ T_e = \varphi_d i_q - \varphi_q i_d \end{cases} \tag{15}$$

where the parameters are defined as follows:

i_D, i_Q: direct and transverse dampers currents;
T_m, T_e: mechanical and electric torque;
φ_D, φ_Q: direct and transverse dampers total flux;
Φ_{abc}, φ_f: stator and main field total flux;
r_s, r_f, and r_D and r_Q: stator, main field, and dampers resistances;
V_{abc}, I_{abc}: output voltages and armature currents;
v_f, i_f: main field excitation voltage and main field current;
L_D, L_Q: inductances of the direct and quadrature damper windings;
L_f: inductance of the main field winding;
L_d, L_q: inductances of the d-axis stator winding and q-axis stator winding;
m_{sf}: mutual inductance between the field winding and the d-axis stator winding;
m_{sD}: mutual inductance between the d-axis stator winding and the d-axis damper winding;
m_{sQ}: mutual inductance between the q-axis stator winding and the q-axis damper winding;
m_{fD}: mutual inductance between the field winding and the d-axis damper winding.

In (14), v_f and T_m are the control inputs adopted in this work.

3 Controller Design and Analysis

In this section, two nonlinear robust controllers designed for PVs and BESSs are presented. These proposed novel design methods are based on the control constraints. For SG, a super-twisting integral SMC is designed to regulate the SG. It is assumed that there are precise internal oscillators and an open-loop strategy [5] is adopted to control the phase and frequency.

3.1 Controller Design for PV

In this subsection, a novel Lyapunov based controller inspired by the SMC strategy is proposed for PV. Although this controller is inspired by the SMC strategy, it does not have a sliding surface and it has different features. An important goal in the controller design for PV is to maximize the output power. There are different approaches to get maximum power from PVs which are referred to as maximum power point tracking (MPPT) methods. According to (2), only two control inputs are available while the system has three independent states. Therefore, two desired outputs can be defined for the system. In [2], a controller is designed and presented for a PV to generate desired active and reactive power outputs. As both desired power outputs are considered, it is not possible to track the maximum power point (MPP). It is therefore assumed that the MPP (v_{pv}^{ref}, i_{pv}^{ref}) is given and the controller task is to follow this point. This can be achieved by MPPT. Working at MPP sets the active output power to the maximum power. It is indeed appealing to generate a desired reactive power as well. As arbitrary reactive power generation is not possible, an algorithm is proposed to produce the closest possible reactive power to the desired value using inverter switch signals.

Assuming E_d = 0, the derivatives of the states at the equilibrium (steady-state condition) become zero and, thus, the following relations hold,

$$\begin{cases} 0 = -\dfrac{R}{L} I_d^{ref} + \omega I_q^{ref} + \dfrac{v_{pv}^{ref}}{L} K_d \\ 0 = -\omega I_d^{ref} - \dfrac{R}{L} I_q^{ref} - \dfrac{E_q}{L} + \dfrac{v_{pv}^{ref}}{L} K_q \\ 0 = \dfrac{1}{C} i_{pv}^{ref} - \dfrac{1}{C}\left(I_d^{ref} K_d + I_q^{ref} K_q\right) \end{cases} \tag{16}$$

where I_d^{ref}, I_q^{ref}, v_{pv}^{ref} and i_{pv}^{ref} are the reference values, and the system is settled at the desired values. In (16), it is assumed that v_{pv}^{ref} and i_{pv}^{ref} are known using an MPPT algorithm. Therefore, the unknown variables I_d^{ref}, I_q^{ref}, K_d, and K_q must be determined. From the first two equations in (16), it can be concluded that,

$$\begin{bmatrix} I_d^{ref} \\ I_q^{ref} \end{bmatrix} = \frac{1}{R^2+L^2\omega^2}\begin{bmatrix} R & L\omega \\ -L\omega & R \end{bmatrix}\begin{bmatrix} v_{pv}^{ref}K_d \\ v_{pv}^{ref}K_q - E_q \end{bmatrix} \tag{17}$$

By substituting (17) in the last equation of (16), (18) is obtained.

$$i_{pv}^{ref} = \frac{Rv_{pv}^{ref}}{R^2+L^2\omega^2}(K_d^2+K_q^2) - \frac{L\omega K_d + RK_q}{R^2+L^2\omega^2}E_q \tag{18}$$

It can be concluded from (17) that,

$$I_d^{ref} = \frac{L\omega v_{pv}^{ref}}{R^2+L^2\omega^2}\left(\frac{R}{L\omega}K_d + K_q - \frac{E_q}{v_{pv}^{ref}}\right) \tag{19}$$

Therefore, the following optimization problem is suggested to define unknown variable values in steady-state.

$$\min_{K_d,K_q} |Q - Q_d|, \quad -\frac{1}{3} \le K_d, K_q \le \frac{1}{3}$$

$$s.t. \quad i_{pv}^{ref} = \frac{Rv_{pv}^{ref}}{R^2+L^2\omega^2}(K_d^2+K_q^2) - \frac{L\omega K_d + RK_q}{R^2+L^2\omega^2}E_q \tag{20}$$

where Q_d is the desired reactive power. This optimization problem determines the system steady-state and control signals which are referred to as K_{d0} and K_{q0}. The solution of this optimization problem has feasible steady-state control signals at the MPP and minimizes the difference between the generated reactive power and its desired value, i.e. Q_d.

Assuming that $(v_{pv}^{ref}, i_{pv}^{ref})$ is known and the optimization problem of (20) has a solution, system (2) with control signals $K_d = K_{d0}$ and $K_q = K_{q0}$ is globally asymptotically stable and the PV works at the MPP. Fig. 3 illustrates how PV interacts with the microgrid.

The current and voltage regulation errors are defined as (21).

$$\begin{cases} e_{I_d} = I_d^{ref} - I_d \\ e_{I_q} = I_q^{ref} - I_q \\ e_{v_{pv}} = v_{pv}^{ref} - v_{pv} \\ e_{i_{pv}} = i_{pv}^{ref} - i_{pv} \end{cases} \tag{21}$$

Considering (2), the error dynamics can be expressed as below,

$$\begin{cases} \dot{e}_{I_d} = \dot{I}_d^{ref} + \frac{R}{L}I_d - \omega I_q - \frac{v_{pv}}{L}K_{d0} \\ \dot{e}_{I_q} = \dot{I}_q^{ref} + \omega I_d + \frac{R}{L}I_q + \frac{E_q}{L} - \frac{v_{pv}}{L}K_{q0} \\ \dot{e}_{v_{PV}} = \dot{v}_{pv}^{ref} - \frac{1}{C}i_{pv} + \frac{1}{C}\left(I_d K_{d0} + I_q K_{q0}\right) \end{cases} \tag{22}$$

Using (16), (23) yields from (22).

$$\begin{cases} \dot{e}_{I_d} = -\frac{R}{L}e_{Id} + \omega e_{Iq} + \frac{e_{v\,pv}}{L}K_{d0} \\ \dot{e}_{I_q} = -\omega e_{Id} - \frac{R}{L}e_{Iq} + \frac{e_{v\,pv}}{L}K_{q0} \\ \dot{e}_{v_{pv}} = -\frac{\gamma}{C}e_{v\,pv} - \frac{K_{d0}}{C}e_{Id} - \frac{K_{q0}}{C}e_{Iq} \end{cases} \tag{23}$$

In the above relation, $e_{v\,pv}$ and $e_{i\,pv}$ are implicitly related; as PV voltage increases, its current decreases monotonically and vice versa. This suggests that $e_{i\,pv} = -\gamma e_{v\,pv}$ with a positive variable γ. Consider $V(E)$ as a Lyapunov candidate,

$$V(E) = E^T P E \tag{24}$$

in which,

$$P = P^T = \frac{1}{2}\begin{bmatrix} L & 0 & 0 \\ 0 & L & 0 \\ 0 & 0 & C \end{bmatrix} > 0,$$
$$E^T = \begin{bmatrix} e_{Id} & e_{Iq} & e_{v\,pv} \end{bmatrix} \tag{25}$$

where L and C are the PV model inductor and capacitor values, respectively.

The derivative of this Lyapunov function is as follows.

$$V(E) = -E^T Q E, \; Q = \begin{bmatrix} R & 0 & 0 \\ 0 & R & 0 \\ 0 & 0 & \gamma \end{bmatrix} > 0 \tag{26}$$

The negative definiteness of the Lyapunov function guarantees the global asymptotic stability of this system.

It has thus been proven that feasible control signals $K_d = K_{d0}$ and $K_q = K_{q0}$ stabilize the system in MPP. It is worth noting that this system is globally exponentially stable if $\gamma = 0$ is considered, which is trivial using linear control theories. Assuming that $K_d = K_{d0} + K_{d1}$ and $K_q = K_{q0} + K_{q1}$ are feasible control signals with $|K_{d1}| \le \gamma_1$ and $|K_{q1}| \le \gamma_2$. γ_1 and γ_2 can be zero in rare cases where $|K_{d0}| = ⅓$ or $|K_{q0}| = ⅓$. To prevent the occurrence of these cases, it can be assumed that $-⅓ + \varepsilon \le K_d$,

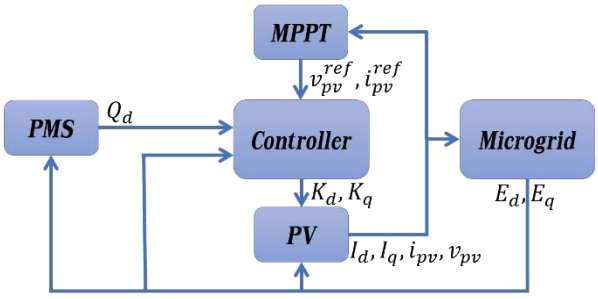

Fig. 3 PV interaction with the microgrid.

$K_q \leq ⅓ - \varepsilon$, where $\varepsilon > 0$ is a small constant, e.g. 0.05. Consequently, $\dot{V}(E)$ for this system becomes as follows,

$$\dot{V}(E) = -\mathrm{Re}_{I_d}^2 - \mathrm{Re}_{I_q}^2 - \gamma e_{I_{v_{pv}}}^2 + f_d K_{d1} + f_q K_{q1} \tag{27}$$

with

$$f_d = e_{v_{pv}} I_d - e_{Id} v_{pv} \tag{28}$$

$$f_q = e_{v_{pv}} I_q - e_{Iq} v_{pv} \tag{29}$$

where $f_d K_{d1}$ and $f_q K_{q1}$ have to be negative for the sake of negative definiteness of the derivative of the Lyapunov function. In addition, these control signals should satisfy their constraints which are $|K_{d1}| \leq \gamma_1$ and $|K_{q1}| \leq \gamma_2$. Inspired by the SMC strategy, it is suggested that $K_{d1} = -\gamma_1 \operatorname{sign}(f_d)$ and $K_{q1} = -\gamma_2 \operatorname{sign}(f_q)$.

By defining the globally stabilizing control signals $K_d = K_{d0} - \gamma_1 \operatorname{sign}(f_d)\alpha$ and $K_q = K_{q0} - \gamma_2 \operatorname{sign}(f_q)\alpha$ with α function as,

$$\alpha = sat_0^1(\gamma_3 \left(\left| e_{Id} \right| + \left| e_{Iq} \right| + \left| e_{v_{pv}} \right| \right), \quad \gamma_3 > 0 \tag{30}$$

for which $sat_0^1(.)$ is a saturation function defined as,

$$sat_0^1(\xi) = \begin{cases} 0 & if \ \xi < 0 \\ \xi & if \ 0 \leq \xi \leq 1 \\ 1 & if \ 1 < \xi \end{cases} \tag{31}$$

and using (27), the Lyapunov derivative becomes as expressed in (32).

$$\dot{V} = -Re_{I_d}^2 - Re_{I_q}^2 - \gamma e_{I_{v_{pv}}}^2 - \gamma_1 \left| f_d \right| \alpha - \gamma_2 \left| f_q \right| \alpha \tag{32}$$

The system with $K_{d1} = K_{q1} = 0$ was globally asymptotically stable and the above reasoning shows that the above control signal definition makes Lyapunov derivative more negative. Therefore, the system remains asymptotically stable and control signals meet their constraints.

The proposed controller has many advantages. The control signals are feasible and guarantee global asymptotic stability. In addition, system robustness is fortified by making the derivative of the Lyapunov function more negative. The suggested controller uses sign function which makes the system robust, similar to SMC. α gain is used in the control signals, to reduce the sign function coefficient as the tracking errors converge to zero. In order to prevent fluctuations in the control signals, small γ_1 and γ_2 should be chosen. These design parameters are bounded based on K_d and K_q limitations and K_{d0} and K_{q0}; nevertheless, K_d and K_q can be computed with arbitrary small positive gains, γ_1 and γ_2, and then the resulted control signals are saturated for the sake of feasibility.

3.2 Controller Design for BESS

The controller proposed for BESS is somehow similar to the design presented earlier. The BESS can exchange power with the microgrid in both charging and discharging modes. Therefore, battery charge or discharge current and exchanged active power are known. Hence, the controllers' task is to provide suitable control signals to keep the active power at its desired value and at the same time minimize the reactive power difference with its desired value. In steady-state, (13) can be expressed as follows:

$$\begin{cases} 0 = \dfrac{1}{\tau_1}\left(M_d I_{bd}^{ref} + M_q I_{bq}^{ref} - I_1^{ref} \right) \\ 0 = -\dfrac{R}{L} I_{bd}^{ref} + \omega I_{bq}^{ref} + \dfrac{v_{dc}^{ref}}{L} M_d \\ 0 = -\omega I_{bd}^{ref} - \dfrac{R}{L} I_{bq}^{ref} - \dfrac{E_q}{L} + \dfrac{v_{dc}^{ref}}{L} M_q \end{cases} \tag{33}$$

In (33), I_1^{ref} and v_{dc}^{ref} are assumed to be known; hence, the reference currents I_{bd}^{ref} and I_{bq}^{ref} control signals M_d and M_q are unknown variables. From the last two equations in (33), the currents I_{bd}^{ref} and I_{bq}^{ref} can be computed as presented in (34).

$$\begin{pmatrix} I_{bd}^{ref} \\ I_{bq}^{ref} \end{pmatrix} = \frac{1}{R^2 + L^2\omega^2} \begin{pmatrix} R & L\omega \\ -L\omega & R \end{pmatrix} \begin{pmatrix} v_{dc}^{ref} M_d \\ v_{dc}^{ref} M_q - E_q \end{pmatrix} \tag{34}$$

Using (34) and the first equation of (33), I_1^{ref} is determined as (35).

$$I_1^{ref} = \frac{R v_{dc}^{ref}}{R^2 + L^2\omega^2}\left(M_d^2 + M_q^2 \right) - \frac{L\omega M_d + R M_q}{R^2 + L^2\omega^2} E_q \tag{35}$$

The following optimization problem is therefore suggested to obtain the unknown variable values in steady-state.

$$\min_{M_d, M_q} \left| Q - Q_d \right|, \quad -\frac{1}{3} \leq M_d, M_q \leq \frac{1}{3}$$

$$s.t.$$

$$I_1^{ref} = \frac{R v_{dc}^{ref}}{R^2 + L^2\omega^2}\left(M_d^2 + M_q^2 \right) - \frac{L\omega M_d + R M_q}{R^2 + L^2\omega^2} E_q \tag{36}$$

The above problem minimizes the difference between the generated reactive power and its desired value while it determines steady-state currents and control signals to settle at the steady-state point. The resulted steady-state control signals are referred to as M_{d0} and M_{q0}.

System (13) with constant control signals M_{d0} and M_{q0} is globally asymptotically stable and BESS settles at $v_{dc} = v_{dc}^{ref}$, $I_1 = I_1^{ref}$, $I_{bd} = I_{bd}^{ref}$ and $I_{bq} = I_{bq}^{ref}$. Fig. 4 illustrates how BESS interacts with the microgrid.

By solving similar expressions as for the PV control system, the below relation can be obtained for BESS control systems.

$$\dot{V} = -e_{I_1}^2 - e_{I_{bd}}^2 - e_{I_{bq}}^2 - \alpha_1 |f_{bd}|\beta - \alpha_2 |f_{bq}|\beta \tag{37}$$

where e_{I1}, $e_{bd,}$ and e_{bq} are current regulation error states, and

$$f_{bd} = -\frac{v_{dc}}{L}\left(P_{12}e_{I_1} + P_{22}E_{I_{bd}} + P_{32}e_{I_{bq}}\right) - \frac{I_{bd}}{\tau_1}\left(P_{11}e_{I_1} + P_{12}e_{I_{bd}} + P_{13}e_{I_{bq}}\right) \tag{38}$$

$$f_{bq} = -\frac{v_{dc}}{L}\left(P_{13}e_{I_1} + P_{23}E_{I_{bd}} + P_{33}e_{I_{bq}}\right) - \frac{I_{bq}}{\tau_1}\left(P_{11}e_{I_1} + P_{12}e_{I_{bd}} + P_{13}e_{I_{bq}}\right) \tag{39}$$

$$\beta = sat_0^1\left(\gamma_4\left(\left|e_{I_{bd}}\right| + \left|e_{I_{bq}}\right| + \left|e_{I_1}\right|\right)\right), \quad \gamma_4 > 0 \tag{40}$$

where P_{ij} is the i-th and j-th column of the matrix satisfying the Lyapunov equation, and α_i and γ_i are like to those for PV.

The proposed controller for BESS is feasible and guarantees global asymptotic stability. It has similar features as the PV controller, which was discussed in the former subsection.

3.3 SG Controller Design

The SG controller design aimed at regulating frequency and power is presented next. First, the phase and frequency, which are virtually decoupled from the rest of the system states of (14), are regulated. If the desired phase, δ_d, is known, the tracking errors and the input torque are defined as follows.

$$e_\delta = \delta - \delta_d \tag{41}$$

$$e_\omega = \omega_e - \omega_0 \tag{42}$$

$$T_m = -T_e + \frac{J}{p}u \tag{43}$$

Then, the double integrator error dynamics can be written as follows,

$$\dot{e}_\delta = e_\omega \tag{44}$$

$$\dot{e}_\omega = u \tag{45}$$

An integrator is added for eliminating any phase bias and the linear quadratic regulator (LQR) theory is used to design an optimal control law.

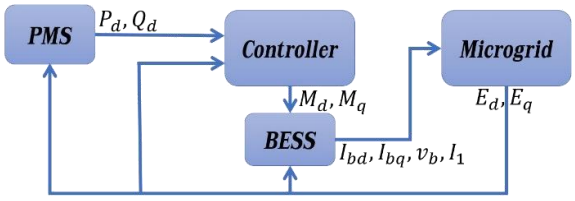

Fig. 4 BESS interaction with the microgrid.

$$\dot{e}_{sg} = \begin{pmatrix} 0 & 1 & 0 \\ 0 & 0 & 1 \\ 0 & 0 & 0 \end{pmatrix} e_{sg} + \begin{pmatrix} 0 \\ 0 \\ 1 \end{pmatrix} u,$$

$$e_{sg}^T = \begin{pmatrix} e_{\delta 0} & e_\delta & e_\omega \end{pmatrix}, \quad e_{\delta 0} = \int_0^t e_\delta dt \tag{46}$$

Then, the controller gains are computed to minimize the following cost function [22].

$$J = \int_0^\infty \left(e_{sg}^T Q_1 e_{sg} + u^T R_1 u\right) dt, Q_1, R_1 > 0 \tag{47}$$

The solution of this optimization problem will be in the form of $u_0 = -Ke_{sg}$. Assuming that the disturbance $d(t)$ is added to the control signal u, the designed integral LQR controller robustness is increased using the super-twisting integral sliding mode control strategy which can eliminate any matched disturbance with a bounded derivative [23]. When $d(t) = 0$ the following system stabilizes the unperturbed system with u_0.

$$\dot{e}_{sg} = \begin{pmatrix} 0 & 1 & 0 \\ 0 & 0 & 1 \\ 0 & 0 & 0 \end{pmatrix} e_{sg} + \begin{pmatrix} 0 \\ 0 \\ 1 \end{pmatrix} \left(u + d\left(t\right)\right), \quad \left|\dot{d}\right| \le \beta \tag{48}$$

The control signal presented in (49) stabilizes (48) in the presence of an unknown time-varying disturbance, $d(t)$.

$$\begin{cases} u = u_0 - \frac{1}{2}\sqrt{|s|}\,\mathrm{sign}\left(s\right) + \rho \\ s = e_\omega\left(t\right) - e_\omega\left(0\right) - \int_0^t u_0 dt \\ \dot{\rho} = -\bar{\beta}\,\mathrm{sign}\left(s\right), \bar{\beta} > \beta \end{cases} \tag{49}$$

In the present work, a robust optimal controller is designed to regulate the SG phase and frequency at their desired values. The remaining dynamics of SG are linear and it is straightforward to prove its stability with a constant v_f.

It is assumed that $E_d = 0$ in the microgrid. However, because of the phase shift δ in SG, dq-voltages obey the following relations.

$$\begin{pmatrix} v_d \\ v_q \end{pmatrix} = \frac{2}{3}\begin{pmatrix} \cos(\omega t + \delta) & \cos\left(\omega t + \delta - \frac{2\pi}{3}\right) & \cos\left(\omega t + \delta + \frac{2\pi}{3}\right) \\ \sin(\omega t + \delta) & \sin\left(\omega t + \delta - \frac{2\pi}{3}\right) & \sin\left(\omega t + \delta + \frac{2\pi}{3}\right) \end{pmatrix} \begin{pmatrix} v_a \\ v_b \\ v_c \end{pmatrix} \tag{50}$$

$$\begin{pmatrix} v_a \\ v_b \\ v_c \end{pmatrix} = \begin{pmatrix} \cos(\omega t) & -\sin(\omega t) \\ \cos\left(\omega t - \frac{2\pi}{3}\right) & -\sin\left(\omega t - \frac{2\pi}{3}\right) \\ \cos\left(\omega t + \frac{2\pi}{3}\right) & -\sin\left(\omega t + \frac{2\pi}{3}\right) \end{pmatrix} \begin{pmatrix} 0 \\ E_q \end{pmatrix} \tag{51}$$

The above equations lead to the following relation between dq-voltages of the grid and SG.

$$\begin{pmatrix} v_d \\ v_q \end{pmatrix} = \begin{pmatrix} v_q \cos(\delta) \\ v_q \sin(\delta) \end{pmatrix} \tag{52}$$

Therefore, the SG active and reactive powers in steady-state are computed as follows.

$$\begin{pmatrix} P_{sg} \\ Q_{sg} \end{pmatrix} = -\frac{1.5E_q^2}{r_s^2 + \omega_0^2 L_q^2 L_d^2} \begin{pmatrix} F_1 \\ F_2 \end{pmatrix}$$
$$\begin{pmatrix} F_1 \\ F_2 \end{pmatrix} = \begin{pmatrix} r_s - 0.5\omega_0 (L_d - L_q)\sin(2\delta) - \frac{\omega_0 m_{sf} v_f}{r_f E_q}(\omega_0 L_q \sin(\delta) + r_s \cos(\delta)) \\ \omega_0 L_q + \omega_0 (L_d - L_q)\sin^2(\delta) - \frac{\omega_0 m_{sf} v_f}{r_f E_q}(\omega_0 L_q \cos(\delta) - r_s \sin(\delta)) \end{pmatrix} \tag{53}$$

Consequently, desired v_f and δ values can be obtained from (52) as the desired active and reactive powers of SG are given. The designed robust optimal controller is able to eliminate the described matched uncertainties and any bias in phase regulation. Fig. 5 illustrates how SG interacts with the microgrid.

4 Numerical Simulations

Four scenarios are considered to show the proposed controller stability and performance. In the first three scenarios, the proposed controllers for PV, BESS, and SG are separately simulated. Then, in the last scenario, a microgrid with two PVs, two BESSs, and one SG is simulated to show how the controllers interact. It is worth noting that the microgrid stability in islanded mode is not considered and it has just been proven that each DER is stable when the grid voltage is at its desired operating point; nevertheless, the simulation results for the last scenario prove that the islanded microgrid is stable as well.

4.1 PV Simulation

The PV parameters and proposed control strategy values used in the calculations are given in Table 1 and (50) and the numerical simulation results are presented in Fig. 6. A very short system transient time (less than 50ms) is seen, and the desired voltage and currents are tracked. This indicates that the system is working at MPP which indicates that the method is implementable as the control signals are within their feasible bounds. It is worth noting that although control signals are non-continuous, the implementation is possible simply because the actuators are inverter switches. The system investigated here is similar to the system simulated in [2]. However, in [2] the control signals were not only out of their feasible range, but they were also sometimes non-definite because the proposed controller becomes singular for zero v_{pv} or I_q.

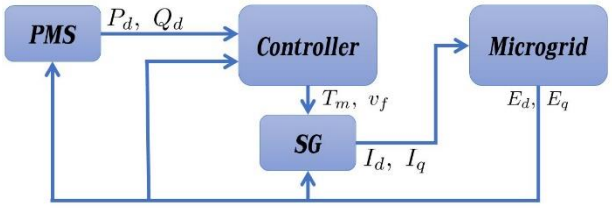

Fig. 5 SG interaction with the microgrid.

$$\begin{pmatrix} I_d^{ref} \\ I_q^{ref} \end{pmatrix} = \begin{pmatrix} -280.541 \\ 70.648 \end{pmatrix}, \begin{pmatrix} K_{d0} \\ K_{q0} \end{pmatrix} = \begin{pmatrix} -0.333 \\ -0.286 \end{pmatrix}, \begin{pmatrix} \gamma_1 \\ \gamma_2 \\ \gamma_3 \end{pmatrix} = \begin{pmatrix} 0.05 \\ 0.05 \\ 0.05 \end{pmatrix} \tag{54}$$

In Fig. 6, the effectiveness of the proposed PV controller in converging the currents and voltages to their reference signals is depicted. It is also noted that the control signals are within their feasible bounds.

4.2 BESS Simulation

BESS and corresponding controller parameters used in the second scenario are presented in Table 2, (51) and (52). The numerical simulation results are presented in Fig. 7.

$$\begin{pmatrix} I_{bd}^{ref} \\ I_{bq}^{ref} \end{pmatrix} = \begin{pmatrix} -126.583 \\ 56.723 \end{pmatrix}, \begin{pmatrix} M_{d0} \\ M_{q0} \end{pmatrix} = \begin{pmatrix} -0.237 \\ 0.333 \end{pmatrix}, \begin{pmatrix} \alpha_1 \\ \alpha_2 \\ \gamma_4 \end{pmatrix} = \begin{pmatrix} 0.08 \\ 0.08 \\ 0.05 \end{pmatrix} \tag{55}$$

Table 1 PV parameters used in the calculations.

Parameter	Value	Parameter	Value
R	0.1 Ω	T_{ref}	*322 K*
L	0.01 H	K_i	0.003 A/K
C	0.0001 F	T_c	298 K
E_g	1.11 eV	k	1.38×10^{-23} J.K^{-1}
E_q	660 V	q	1.6×10^{-19} C
I_{sc}	3.8 A	R_{sh}	1365 Ω
N_p	20	R_s	0.21 Ω
N_s	20	I_{rs}	10^{-11} A
v_{pv}^{ref}	*750 V*	s	1000 W/m^2
i_{pv}^{ref}	73.34 A	A	1.2

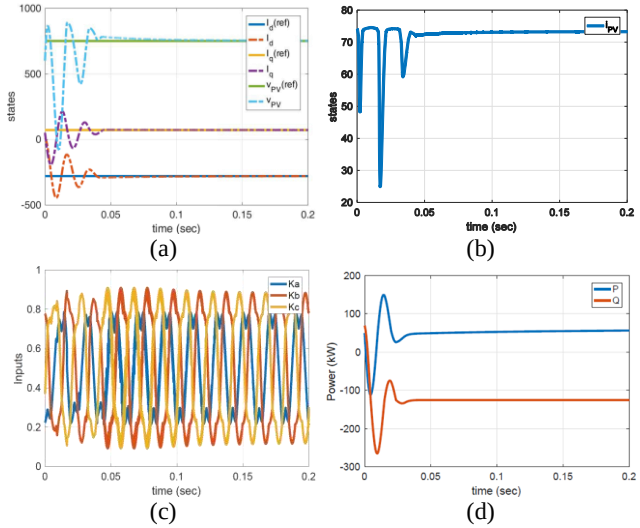

Fig. 6 PV simulation results; a) PV states, b) PV current, c) Control signals in abc-frame, and d) Generated power by PV.

Table 2 BESS parameters.

Parameter	Value	Parameter	Value	Parameter	Value	Parameter	Value
R	0.1 Ω	δ^*	1.4	ε	1.29	C_θ	15 Wh/°C
L	0.01 H	E_{m0}	804.6 V	θ_f	-40 °C	R_θ	0.2 °C/W
C	0.0001F	K_E	5.8×10^{-4} V/°C	C_0^*	261.9 Ah	R_{20}	0.015 Ω
I^*	49 A	θ_a	25 °C	K_c	1.18	A_{22}	-8.45
R_{10}	0.0007Ω	A_0	-0.3	τ_1	5000 s	A_{21}	-0.8

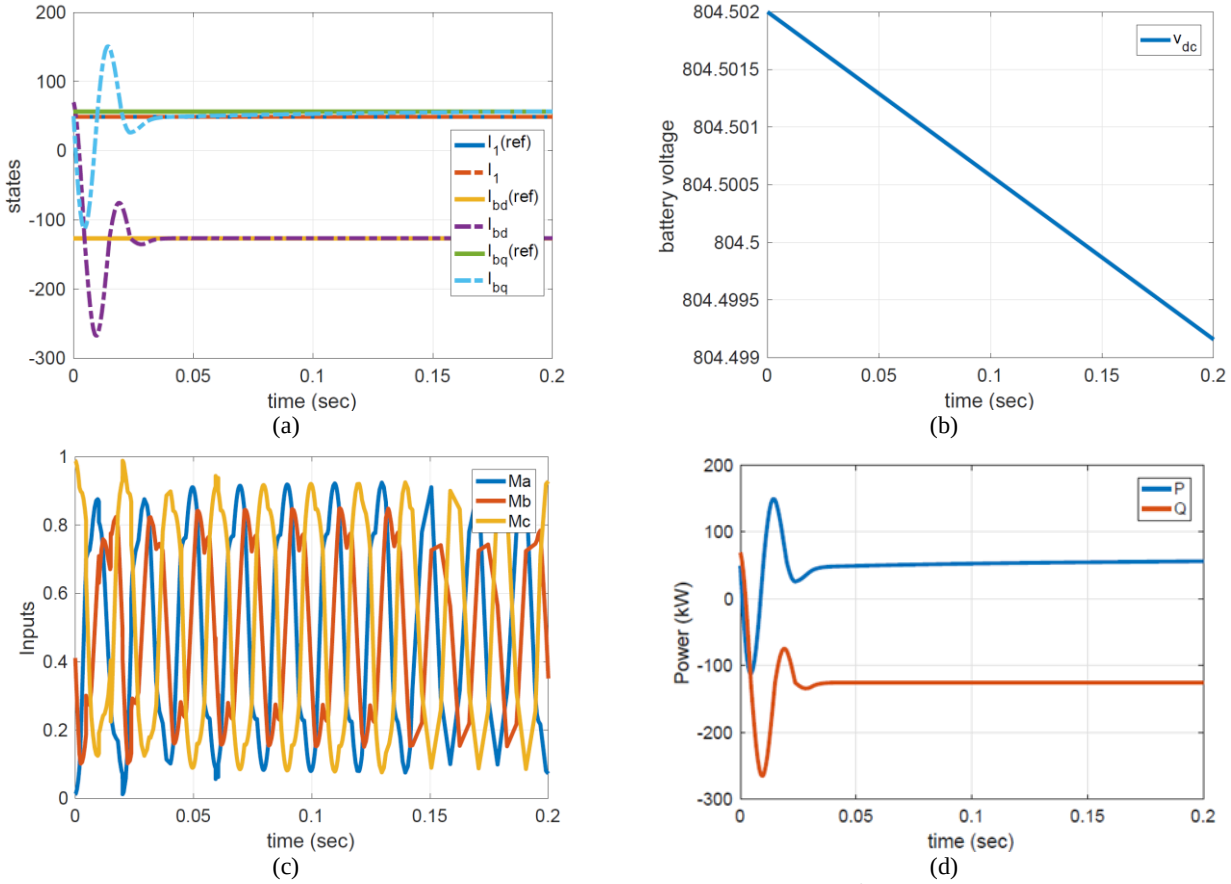

Fig. 7 BESS simulation results; a) BESS states, b) BESS voltage, c) Control signals in abc-frame, and d) Generated power by BESS.

$$P = \begin{pmatrix} 250 & -0.0013 & -3.2942\times10^{-4} \\ -0.0013 & 0.05 & 0 \\ -3.2942 & 0 & 0.05 \end{pmatrix} \tag{56}$$

Fig. 7 validate the effectiveness and fast convergence of the proposed controller. As shown in Fig. 7(a), the desired signals converge in less than 50ms. Also, the control signals are within feasible bounds. BESS voltage is slowly decreasing, which indicates that the battery is discharging, as expected. It is clear that control signals are suitable and the designed controller is implementable.

4.3 SG Simulation

In this subsection, the simulation results for an SG are presented. It is assumed that a three-phase load is connected to the generator and the load value is calculated using the desired active and reactive powers with the desired voltage. SG simulation results are presented in Fig. 8, where it is seen that the system successfully generates the desired power and regulates the phase and frequency.

It can be concluded from Fig. 8 that the proposed method converges very well to reference values, without too much overshoot within a reasonable time frame.

4.4 Microgrid Simulation

Finally, an islanded microgrid consisting of two PVs, two BESSs, and one SG is considered. The microgrid load is connected in parallel with the DERs and is considered to be 700 kW with 0.8 power factor. Therefore, the microgrid reactive power is 525kVar and with E_d = 0V and E_q = 660V as desired voltages in the dq-frame and the load impedance should be Z_L = 0.5974 + j0.4480 Ω. It is assumed that the active load increases to 800 kW and the reactive power decreases to 325kVar at t = 2s, which results in a new load impedance of

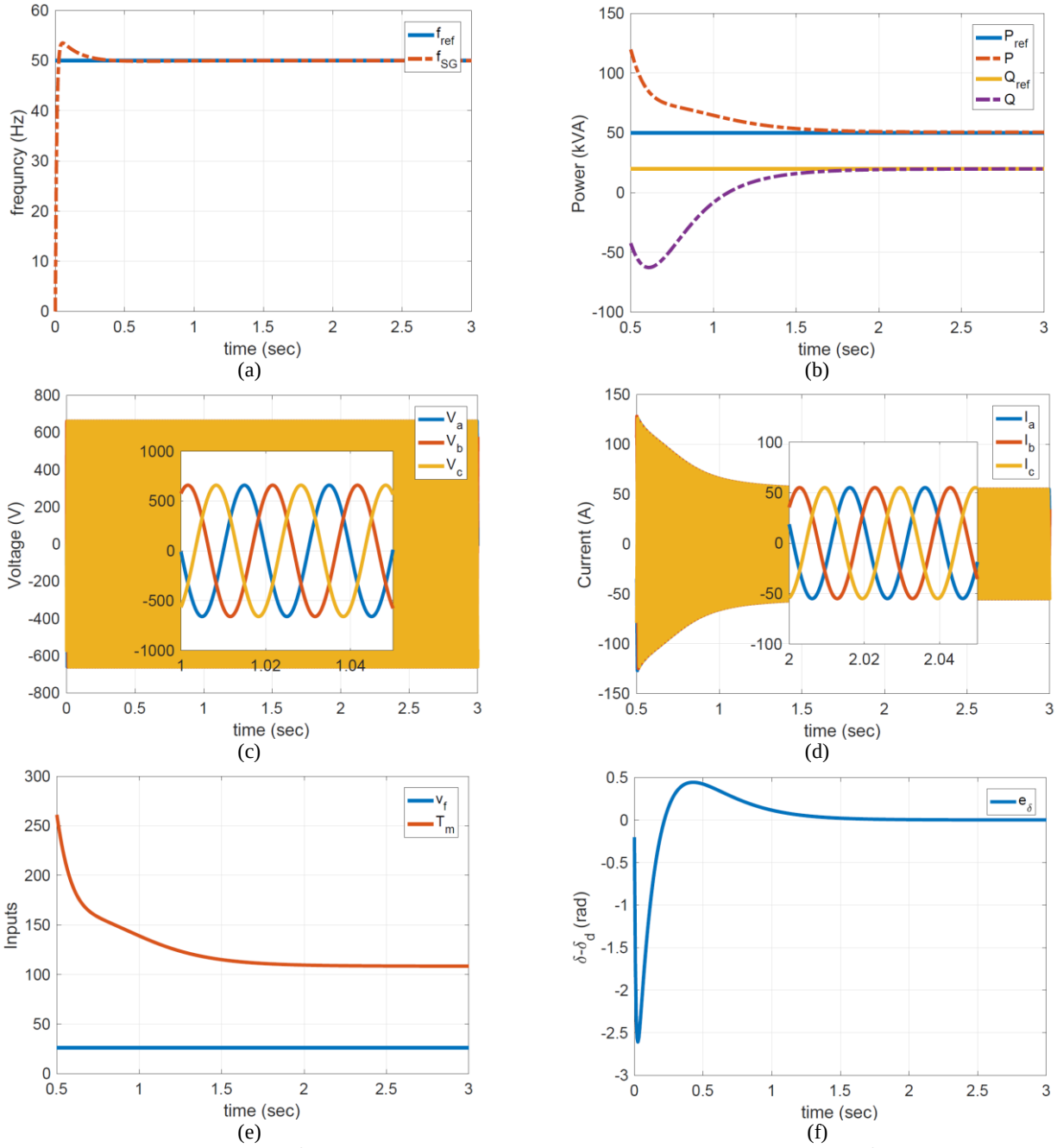

Fig. 8 SG simulation results; a) SG frequency regulation, b) SG power regulation, c) SG voltages in abc-frame, d) SG currents in abc-frame, e) SG control signals, and f) Phase error in SG.

Z_L = 0.7010 + j0.2848 Ω.

All proposed controllers for PV, BESS, and SG are local, which require a PMS to generate reference signals for the local controllers as voltage regulation is considered. The proposed PV controller needs the reference voltage and current points, which can be estimated using an MPPT algorithm. It is assumed that $i_{pv}^{ref} = 73.34A$, $v_{pv}^{ref} = 750V$, and Q_d = 0VAR are PV reference signals. The controller and the nominal PV parameters are the same as in section 4-1. Further, the BESS parameters are as presented in 4-2. The desired SG power generation is determined as the difference between the total supplied powers of the PVs and the BESSs, and the overall microgrid consumption. The simulation results for this scenario are presented in Fig. 9, where the DERs' initial conditions are assumed to be zero.

In Fig. 9, a good tracking of the reference frequency, voltage, and currents with reasonable overshoots, even as the active and reactive load change, is seen. The frequency and load voltage overshoots as the load changes are less than 0.3% and 2.3%, respectively.

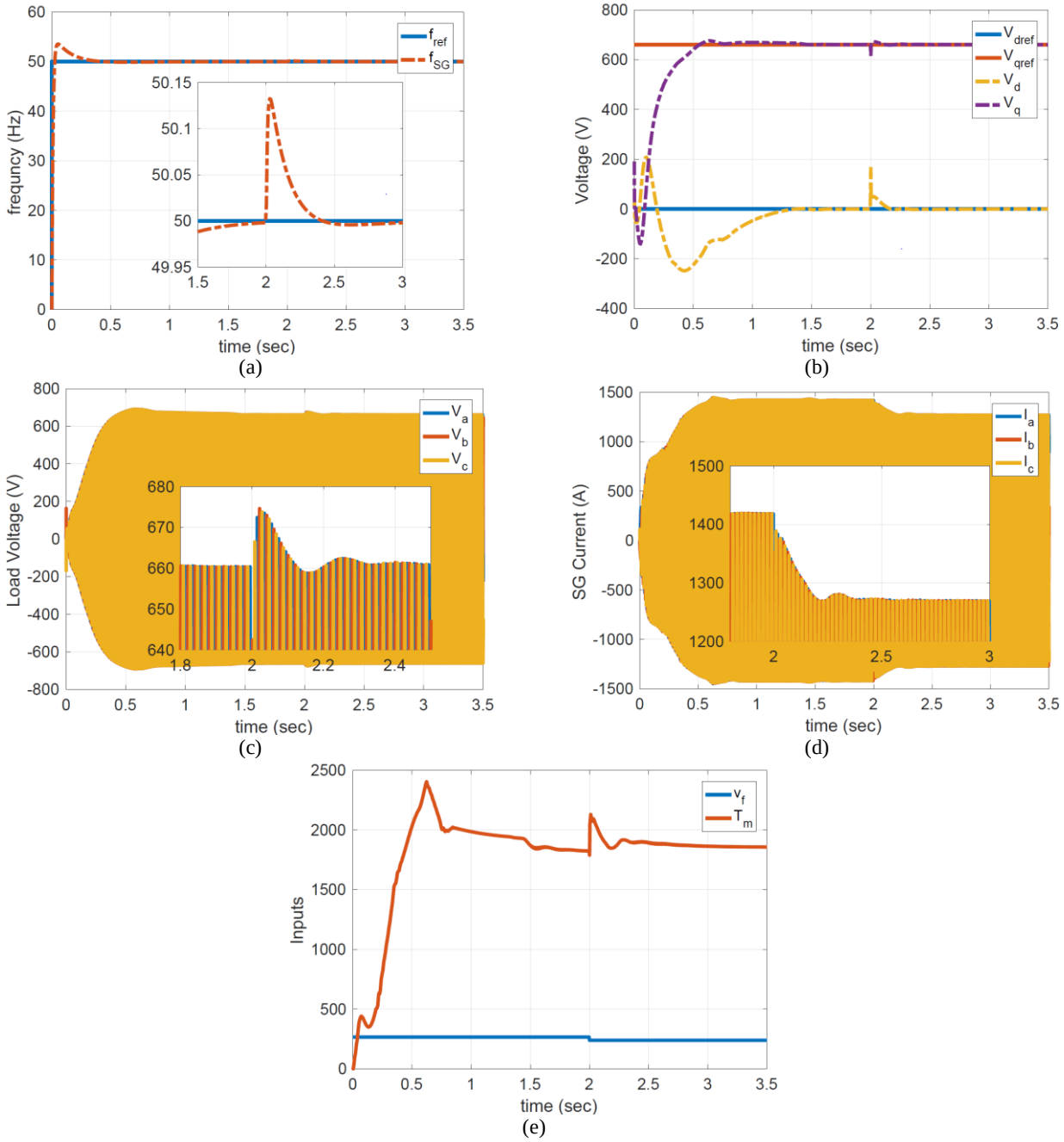

Fig. 9 Microgrid simulation results; a) SG frequency regulation, b) Load voltages in dq-frame, c) Load voltages in abc-frame, d) SG control signals, and e) SG control signals.

5 Conclusions and Future Works

In this paper, distributed nonlinear robust controllers are proposed for PV, BESS, and SG. Along with the robustness and global stability of the proposed controllers, suitable control signals missing in previous related publications were accounted for. In the proposed method, advanced control strategies like nonlinear theories, Lyapunov based design, SMC and its higher order version, perturbation theories, and optimal control strategies were creatively combined to control each DER in an islanded microgrid. A load change was investigated by simulation, which showed that the proposed controller is robust against these changes.

For future works, the authors are going to implement phase difference as a control input to the proposed PV and BESS controllers, which is similar to what was used to control the SG in this study. Another goal is to adopt MPPT for PV and show how it matches with the controller and PMS. In this paper, it is assumed that the target current and voltage values for PVs are known, and in future studies, the authors are going to integrate an MPPT strategy to the proposed controller. Finally, as measurement and actuator delays affecting stability

analysis exist in microgrids the authors would like to address this in future studies.

References

[1] Z. A. Arfeen, A. B. Khairuddin, R. M. Larik, and M. S. Saeed, "Control of distributed generation systems for microgrid applications: A technological review," *International Transactions on Electrical Energy Systems*, Vol. 29, No. 9, p. e12072, 2019.

[2] M. A. Mahmud, M. J. Hossain, H. R. Pota, and A. M. T. Oo, "Robust nonlinear distributed controller design for active and reactive power sharing in islanded microgrids," *IEEE Transactions on Energy Conversion*, Vol. 29, No. 4, pp. 893–903, 2014.

[3] M. Babazadeh and H. Karimi, "Robust decentralized control for islanded operation of a microgrid," in *Power and Energy Society General Meeting*, Detroit, USA, pp. 1–8, 2011.

[4] M. Babazadeh and H. Karimi, "A robust two-degree-of-freedom control strategy for an islanded microgrid," *IEEE Transactions on Power Delivery*, Vol. 28, No. 3, pp. 1339–1347, 2013.

[5] A. H. Etemadi, E. J. Davison, and R. Iravani, "A decentralized robust control strategy for multi-der microgrids part I: Fundamental concepts," *IEEE Transactions on Power Delivery*, Vol. 27, No. 4, pp. 1843–1853, 2012.

[6] A. H. Etemadi, E. J. Davison, and R. Iravani, "A generalized decentralized robust control of islanded microgrids," *IEEE Transactions on Power Systems*, Vol. 29, No. 6, pp. 3102–3113, 2014.

[7] H. Bevrani, M. R. Feizi, and S. Ataee, "Robust frequency control in an islanded microgrid: H_∞ and μ-synthesis approaches," *IEEE Transactions on Smart Grid*, Vol. 7, No. 2, pp. 706–717, 2016.

[8] M. Mahmud, H. Pota, and M. Hossain, "Dynamic stability of three-phase grid-connected photovoltaic system using zero dynamic design approach," *IEEE Journal of Photovoltaics*, Vol. 2, No. 4, pp. 564–571, 2012.

[9] M. Mahmud, H. Pota, and M. Hossain, "Nonlinear controller design for single-phase grid-connected photovoltaic systems using partial feedback linearization," in *2nd Australian Control Conference (AUCC)*, Sydney, Australia, pp. 30–35, 2012.

[10] M. Mahmud, M. Hossain, H. Pota, and N. Roy, "Nonlinear distributed controller design for maintaining power balance in islanded microgrids," in *PES General Meeting| Conference & Exposition*, National Harbor, USA, pp. 1–5, 2014.

[11] D. Lalili, A. Mellit, N. Lourci, B. Medjahed, and E. Berkouk, "Input output feedback linearization control and variable step size MPPT algorithm of a grid-connected photovoltaic inverter," *Renewable Energy*, Vol. 36, No. 12, pp. 3282–3291, 2011.

[12] I. S. Kim, "Robust maximum power point tracker using sliding mode controller for the three-phase grid-connected photovoltaic system," *Solar Energy*, Vol. 81, No. 3, pp. 405–414, 2007.

[13] Y. Karimi, H. Oraee, M. S. Golsorkhi, and J. M. Guerrero, "Decentralized method for load sharing and power management in a PV/battery hybrid source islanded microgrid," *IEEE Transactions on Power Electronics*, Vol. 32, No. 5, pp. 3525–3535, 2017.

[14] X. Lu, X. Yu, J. Lai, J. M. Guerrero, and H. Zhou, "Distributed secondary voltage and frequency control for islanded microgrids with uncertain communication links," *IEEE Transactions on Industrial Informatics*, Vol. 13, No. 2, pp. 448–460, 2017.

[15] G. Lou, W. Gu, W. Sheng, X. Song, and F. Gao, "Distributed model predictive secondary voltage control of islanded microgrids with feedback linearization," *IEEE Access*, Vol. 6, pp. 50169–50178, 2018.

[16] L. Sedghi, M. Emam, A. Fakharian, and S. Savagheb, "Decentralized control of an islanded microgrid based on offline model reference adaptive control," *Journal of Renewable and Sustainable Energy*, Vol. 10, No. 6, 2018.

[17] Y. Xu, Q. Guo, H. Sun, and Z. Fei, "Distributed discrete robust secondary cooperative control for islanded microgrids," *IEEE Transactions on Smart Grid*, Vol. 10, No. 4, pp. 3620–3629, 2019.

[18] S. M. Hoseini, N. Vasegh, and A. Zangeneh, "Robust hybrid control of output power for three-phase grid connected PV system," *International Journal of Industrial Electronics, Control and Optimization*, Vol. 2, No. 4, pp. 365–372, 2019.

[19] M. Ceraolo, "New dynamical models of lead-acid batteries," *IEEE Transactions on Power Systems*, Vol. 15, No. 4, pp. 1184–1190, 2000.

[20] A. Barakat, S. Tnani, G. Champenois, and E. Mouni, "Analysis of synchronous machine modeling for simulation and industrial applications," *Simulation Modelling Practice and Theory*, Vol. 18, No. 9, pp. 1382–1396, 2010.

[21] G. Andersson, "Dynamics and control of electric power systems," *Class Lecture*, pp.227-0528, 2012.

[22] D. E. Kirk, *Optimal control theory: an introduction*. Mineola, New York, Dover Publication, 2012.

[23] J. A. Moreno and M. Osorio, "Strict Lyapunov functions for the super-twisting algorithm," *IEEE Transactions on Automatic Control*, Vol. 57, No. 4, pp. 1035–1040, 2012.

S. M. Hoseini was born in Tehran, Iran, in 1983. He received his B.Sc. degree from the Faculty of Engineering, University of Yazd, Yazd, Iran, in 2005 and M.Sc. degree from the Faculty of Engineering, University of Kashan, Kashan, Iran, in 2009. He is now a Ph.D. student at the Faculty of Engineering, University of Shahid Rajaee Teacher Training, Tehran, Iran. His research interests are in distributed generation, microgrid, and power system control.

N. Vasegh received her B.Sc. degree in Electronic Engineering in 2001, and both her M.Sc. degree in 2004 and the Ph.D. degree in 2008 in Control Engineering from K. N. Toosi University of Technology. Since 2011, she has been with Control Engineering Department at Shahid Rajaee Teacher Training University. Her current research interests are in the areas of nonlinear control, and time-delayed systems analysis and control, and application of control theory in power systems.

A. Zangeneh received his Ph.D. degree in Electrical Engineering from Iran University of Science and Technology (IUST) in 2010. He is now an Assistant Professor at the Electrical Engineering Department of Shahid Rajaee Teacher Training University (SRTTU). His research interests are in demand-side management, smart grid, distributed generation, optimization in power systems, and power system resiliency.